Electronic Supplementary Information

A new sodium vanadyl fluorophosphate as high-rate and stable cathode for aqueous hybrid sodium-zinc batteries

Xun Zhao,[a] Lei Mao,[a] Qihui Cheng,[a] Fangfang Liao,[a] Guiyuan Yang,[a] and Lingyun Chen [a] *

[a] School of Chemistry and Chemical Engineering, Chongqing University, Chongqing 400044, P. R. China

*Corresponding author. E-mail: lychen@cqu.edu.cn

Experimental section

Materials preparation: A facile solvothermal method was used to prepare the $Na_x(VO)_2(PO_4)_yF_z$ sample. Simply, 0.7 mL (*ca*. 10 mmol) H_3PO_4, 3.782 g (30 mmol) $H_2C_2O_4{\cdot}2H_2O$, 0.84 g (20 mmol) NaF, and 1.82 g (10 mmol) V_2O_5 were successively added into the mixed solution of 30 mL distilled water and 30 mL absolute ethanol. After stirring for 30 min, the the dispersion solution was transferred into a Teflon-lined stainless-steel autoclave (100 mL, Anhui Kemi Machinery Technology Co., Ltd.) and then heated to 180 °C for 12 h. The as-obtained dark gray products were washed with distilled water for three times and then dried at 80 °C for 12 h. The possible solvothermal reactions of the formation of $Na_x(VO)_2(PO_4)_yF_z$ are listed as the following equations:

$$V_2O_5 + 3H_2C_2O_4 \rightarrow 2VO^{2+} + 2C_2O_4^{2-} + 2CO_2 + 3H_2O \quad (1)$$

$$x\mathrm{Na}^{+} + 2VO^{2+} + y\mathrm{PO}_4^{3-} + z\mathrm{F}^{-} \rightarrow \mathrm{Na}_x(VO)_2(\mathrm{PO}_4)_y\mathrm{F}_z \quad (2)$$

Materials characterization: The crystalline phase of the sample was identified by X-ray diffraction (XRD) and the XRD patterns were recorded by a Bruker D8 Advance powder diffractometer using Cu Kα radiation (λ = 1.5406 Å). Inductively coupled plasma optical emission spectrometer (ICP-OES, Thermo Scientific ICAP 6300) was used to analyze the elemental content of the sample. Thermogravimetric analysis (TGA) was performed to investigate the structrual water content of the sample under Ar gas flow with the heating rate of 5 °C min^{-1} by using a thermal analyzer (Mettler Toledo TGA2). X-ray photoelectron spectroscopy (XPS) experiments were conducted on an ESCALAB 250Xi electron spectrometer. The morphology and dimensions of the sample were observed by scanning electron microscopy (SEM, Quattro S), and field-emission transmission electron microscope (TEM, Talos F200S) was used to characterize the high-resolution TEM (HRTEM) image, selected area electron diffraction (SAED), and element mapping as well as energy dispersive spectrometry (EDS).

Electrochemical measurements: For the preparation of cathode, 10 *wt.*% polyvinylidene fluoride, 20 *wt.*% acetylene black, and 70 *wt.*% active materials were successively dispersed in N-methyl-2-pyrrolidone and the resultant slurry was uniformly pasted onto the titanium foil. After being dried at 80 °C under a vacuum for 12 h, the mass loading of the active materials was about 3.0-4.0 mg cm^{-2}. The "water-in-bisalts" electrolyte, 15 m (mol kg^{-1}) $NaClO_4$ + 1 m $Zn(OTf)_2$, was prepared by adding 10.535 g (75 mmol) $NaClO_4 \cdot H_2O$ into 3.75 mL distilled water under sonication and then 1.818 g (5 mmol) $Zn(OTf)_2$ was added for further sonication time of 30 min. The aqueous hybrid sodium-zinc batteries were assembled in air, in which 15 m $NaClO_4$ + 1 m $Zn(OTf)_2$ "water-in-bisalts" solution, zinc foil, and glass fiber filter (Whatman, GF/D) respectively served as electrolyte, anode, and separator. Galvanostatic charge-discharge (GCD) tests in a potential window of 0.4-2.2 V (*vs*. Zn^{2+}/Zn) were performed with a LAND battery testing system (CT3001A) for studying rate and cyclic performance. Galvanostatic intermittent titration technique (GITT) was employed to determine the Zn^{2+} diffusion coefficient ($D_{Zn^{2+}}$) within a charge/discharge time of 10 min and followed by a relaxation time of 60 min at a current density of 50 mA g^{-1}. Cyclic voltammetry (CV, 0.4-2.2 V) and electrochemical impedance spectroscopy (EIS, 100 kHz to 0.01 Hz) measurements were conducted on a CHI760E electrochemical workstation.

Table S1 The lattice parameters, cell volumes, and atomic sites of the $Na_x(VO)_2(PO_4)_yF_z$.

Symmetry	Tetragonal			
Space group	*I*4/*mmm*			
Lattice parameters	a = 6.392 Å	b = 6.392 Å	c = 10.632 Å	V = 434.433 Å^3
	α = 90°	β = 90°	γ = 90°	
Rp	4.41			
Rwp	5.61			
Rexp	4.90			
Chi2	1.31			
Name	x	y	z	occupancy
V1	0	0	0.19708	0.125
Na2	0.21813	0.50000	0	0.016
Na1	0.27208	0.27208	0	0.172
P1	0	0.50000	0.25000	0.125
O1	0	0.30809	0.16269	0.500
O2	0	0	0.35579	0.125
F1	0	0	0	0.062

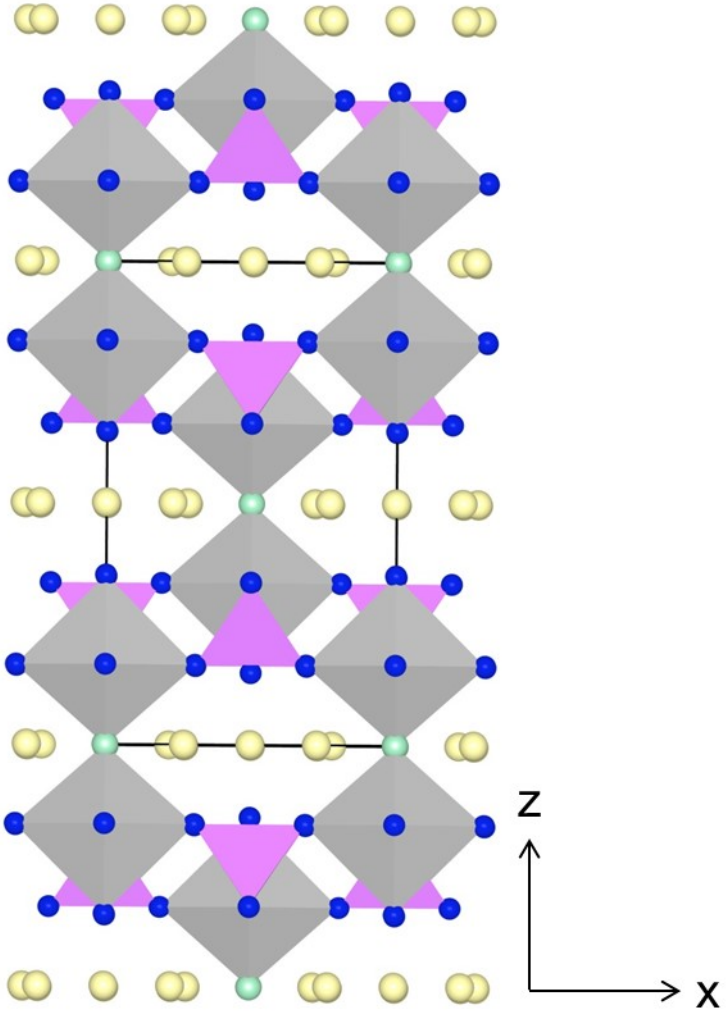

Fig. S1 The crystal structure of $Na(VO)_2(PO_4)_{1.5}F_{0.5}$, in which the sodium, oxygen, and fluorine are respectively yellow, blue, and green, and vanadium and phosphorus are inside the respective gray VO_6 octahedrons and pink PO_4 tetrahedron.

Table S2 The ICP-OES data of the $Na_x(VO)_2(PO_4)_yF_z$.

Element	Detected mass content (%)	Atomic ratio
Na	6.93	1.04
V	29.5	2
P	13.14	1.46

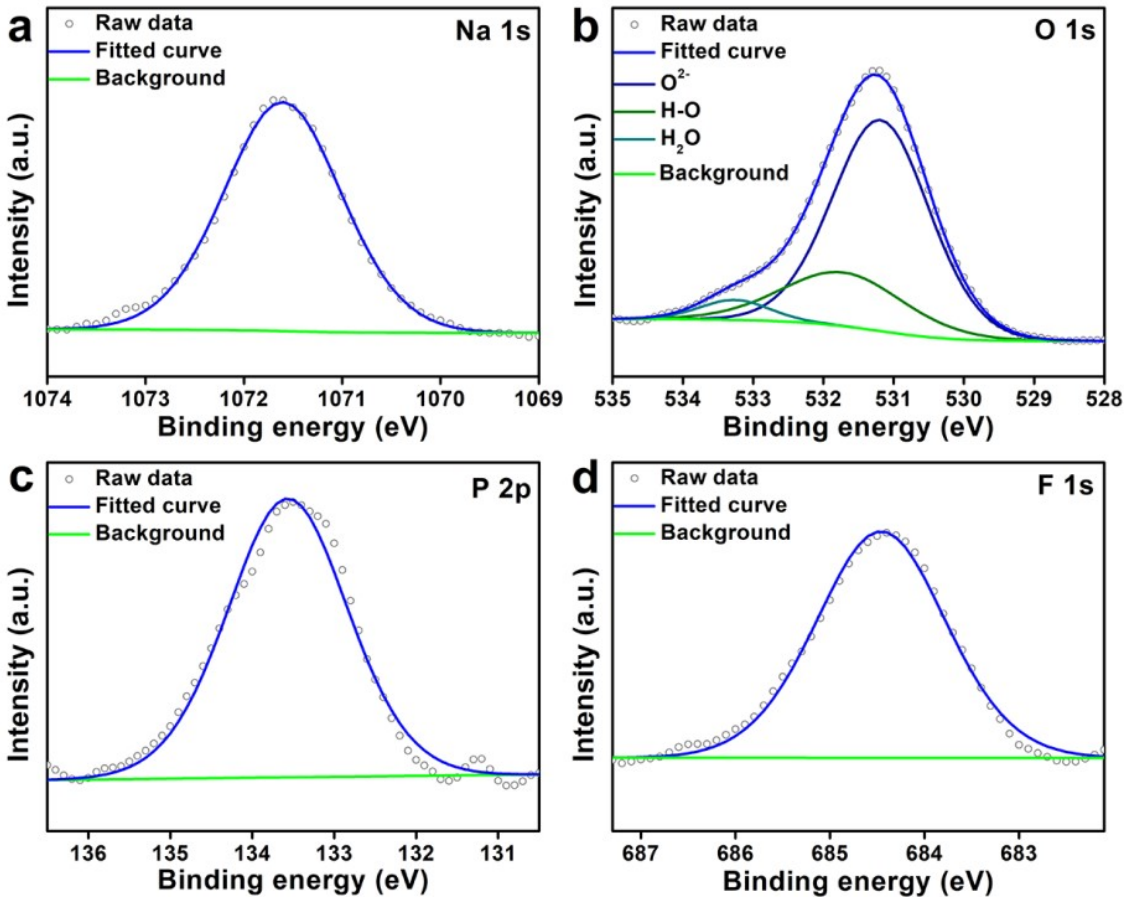

Fig. S2 (a) Na 1s, (b) O 1s, (c) P 2p, and (d) F 1s region of $Na(VO)_2(PO_4)_{1.5}F_{0.5}$.

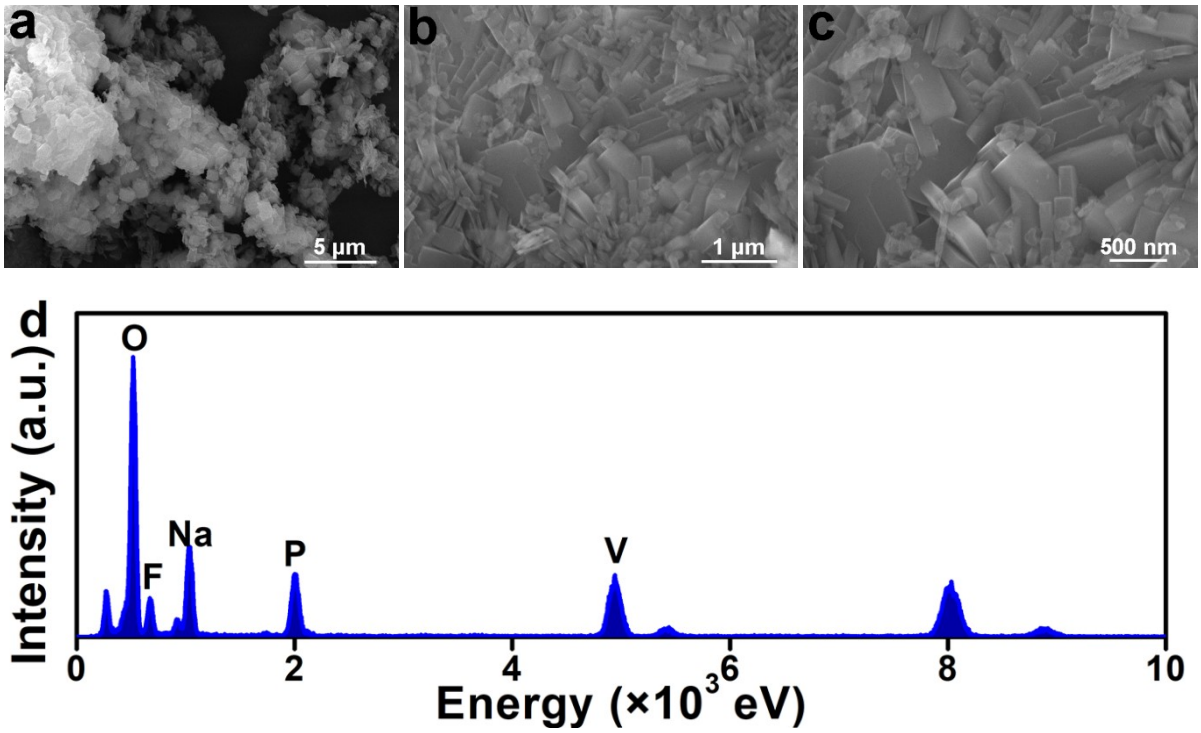

Fig. S3 (a-c) SEM images under different magnification and (d) EDS of $Na(VO)_2(PO_4)_{1.5}F_{0.5}$.

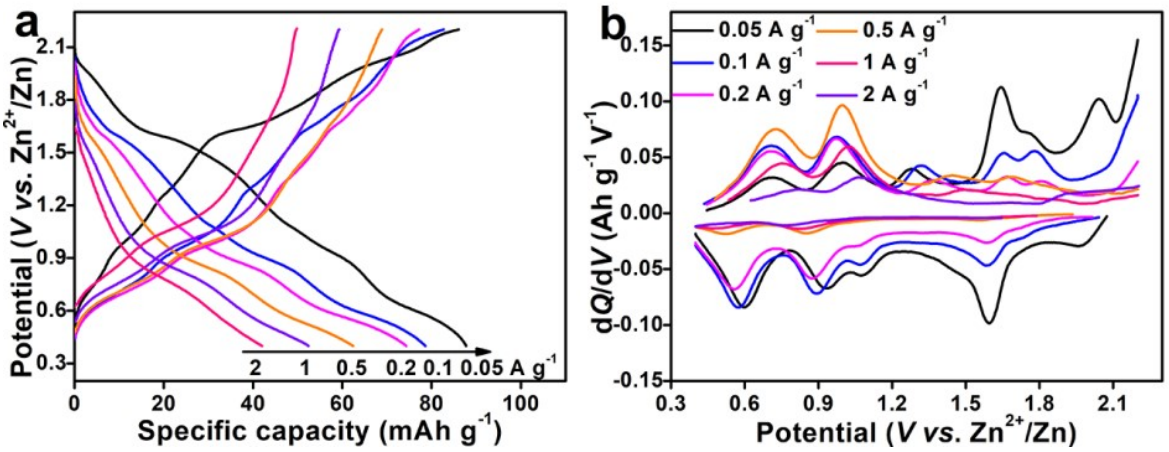

Fig. S4 (a) GCD curves and (b) differential capacity curves of Zn-$Na(VO)_2(PO_4)_{1.5}F_{0.5}$ battery at different current densities from 0.05 to 2 A g^{-1}.

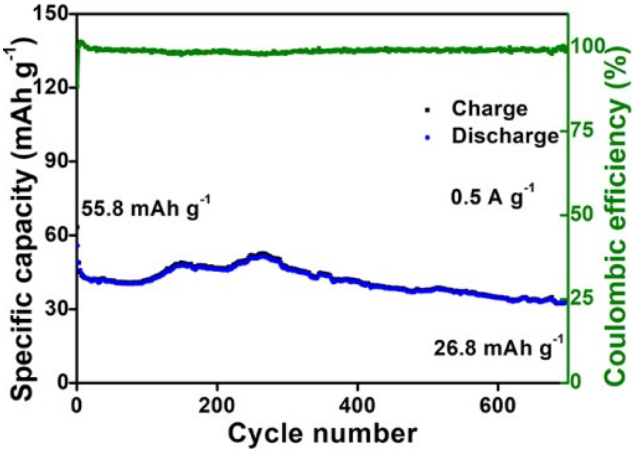

Fig. S5 (a) Cyclic performance and coulombic efficiency of Zn-$Na(VO)_2(PO_4)_{1.5}F_{0.5}$ battery at 0.5 A g^{-1}.

Table S3 Comparison of specific capacity and energy density of $Na(VO)_2(PO_4)_{1.5}F_{0.5}$ as cathode with other advanced vanadium-based phosphate and fluorophosphate cathodes for aqueous batteries

Vanadium-based fluorophosphate cathode	Electrolyte	Specific capacity (current density)	Energy density (Wh kg^{-1})	Power density (W kg^{-1})	Ref.
Carbon-coated $NaVPO_4F$	15 m $NaClO_4$ + 1 m $Zn(CF_3SO_3)_2$	88.9 mAh g^{-1} (0.05 A g^{-1})	113	68	1
$Na_3V_2(PO_4)_2O_{1.6}F_{1.4}$	25 m $ZnCl_2$ + 5 m NH_4Cl	155 mAh g^{-1} (0.05 A g^{-1})	–	–	2
VPO_4F	$ZnCl_2$-$(NH_2)_2CO$ ionic liquid	120 mAh g^{-1} (0.02 C)	–	–	3
$KVOPO_4$	4 m $Zn(CF_3SO_3)_2$	89.2 mAh g^{-1} (0.1 A g^{-1})	–	–	4
PPy-$VOPO_4$	1 M $Zn(CF_3SO_3)_2$/ acetonitrile with 10% vol% water	76 mAh g^{-1} (0.05 A g^{-1})	–	–	5
$H_{0.6}(VO)_3(PO_4)_3 3H_2O$	3 M $ZnSO_4$	50 mAh g^{-1} (0.1 A g^{-1})	–	–	6
$VOPO_4$-Gr heterostructures	1 M $Zn(CF_3SO_3)_2$/ acetonitrile	110 mAh g^{-1} (0.05 A g^{-1})	–	–	7
S-$VOPO_4$	30 m $ZnCl_2$	207 mAh g^{-1} (0.1 A g^{-1})	–	–	8
$Mn_{0.25}(VO)_{0.75}PO_4 \cdot 2H_2O$	3 M $Zn(CF_3SO_3)_2$	207.7 mAh g^{-1} (0.1 A g^{-1})	–	–	9
$Na(VO)_2(PO_4)_{1.5}F_{0.5}$	15 m $NaClO_4$ + 1 m $Zn(CF_3SO_3)_2$	105.9 mAh g^{-1} (0.05 A g^{-1})	130.23	61.5	This work

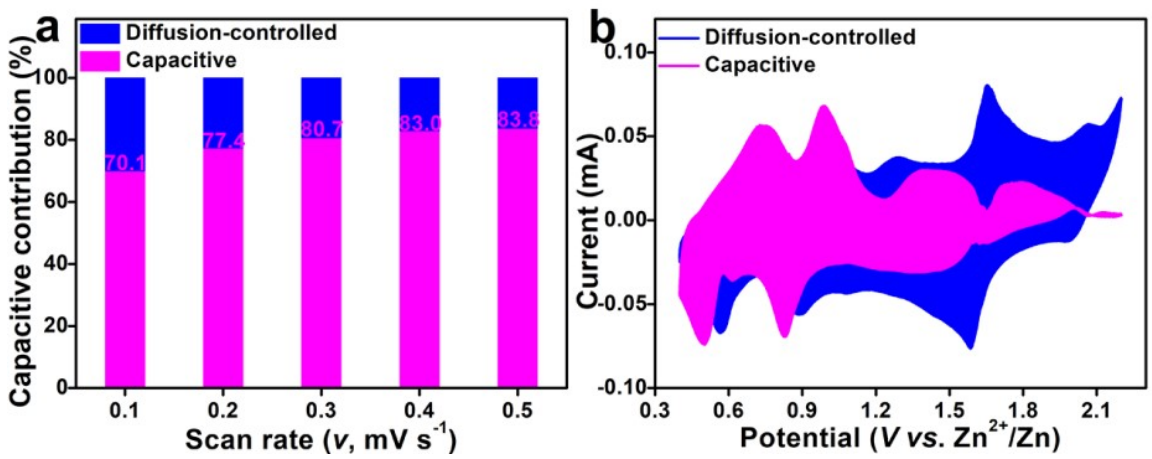

Fig. S6 (a) The surface-controlled capacitive contribution at different scan rate from 0.1 to 0.5 mV s^{-1}; (b) the CV curves containing the capacitive contribution at 0.1 mV s^{-1}.

Table S4 Comparison of the resistance values measured at pristine, 10th, and 4000th cycle.

State	R_s (Ω)	R_{ct} (Ω)	Z_w (Ω)	R_{SEI} (Ω)
Pristine	0.888	494.4	6.227×10^{-3}	1.319
10th cycle	1.364	28.09	1.358×10^{-2}	8.256
4000th cycle	1.408	102.1	1.980×10^{-2}	4.826

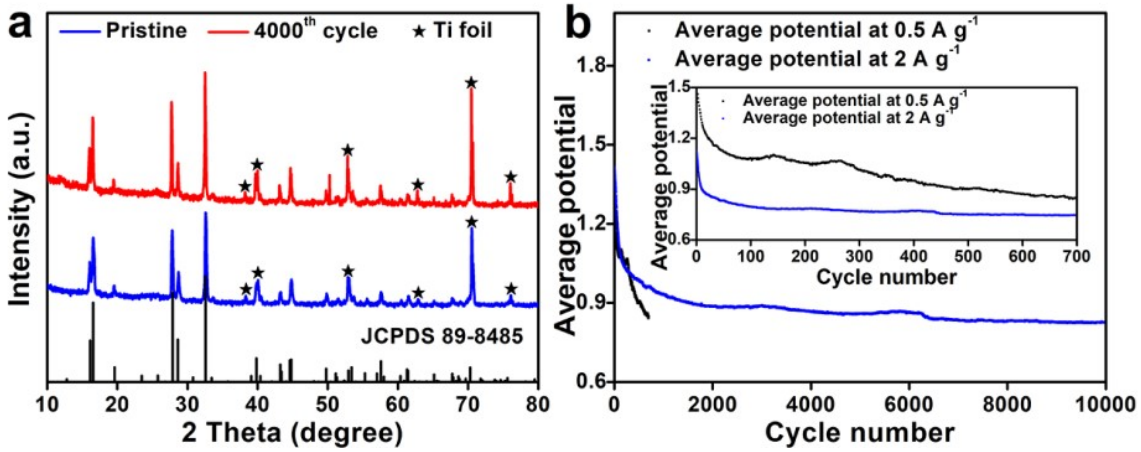

Fig. S7 (a) XRD patterns at pristine state and after 4000 cycles; (b) the average discharge potential at the current density of 0.5 and 2 A g^{-1}.

References

1. Y. Shen, B. Liu, X. Liu, J. Liu, J. Ding, C. Zhong and W. Hu, *Energy Storage Mater.*, 2021, **34**, 461-474.
2. Q. Ni, H. Jiang, S. Sandstrom, Y. Bai, H. Ren, X. Wu, Q. Guo, D. Yu, C. Wu and X. Ji, *Adv. Funct. Mater.*, 2020, **30**, 2003511.
3. H. Yaghoobnejad Asl, S. Sharma and A. Manthiram, *J. Mater. Chem. A*, 2020, **8**, 8262-8267.
4. K. Zhu, Z. Sun, P. Liu, H. Li, Y. Wang, K. Cao and L. Jiao, *J. Energy Chem.*, 2021, **63**, 239-245.
5. V. Verma, S. Kumar, W. Manalastas, J. Zhao, R. Chua, S. Meng, P. Kidkhunthod and M. Srinivasan, *ACS Appl. Energy Mater.*, 2019, **2**, 8667-8674.
6. Y. De Luna and N. Bensalah, *Front. Mater.*, 2021, **8**, 645915.
7. P. Xiong, F. Zhang, X. Zhang, S. Wang, H. Liu, B. Sun, J. Zhang, Y. Sun, R. Ma, Y. Bando, C. Zhou, Z. Liu, T. Sasaki and G. Wang, *Nat. Commun.*, 2020, **11**, 3297.
8. M. Zhang, Y. Pei, R. Liang, R. Gao, Y.-P. Deng, Y. Hu, Z. Chen and A. Yu, *Nano Energy*, 2022, **98**, 107268.
9. J. Guo, W. Ma, Z. Sang, X. Zhang, J. Liang, F. Hou, W. Si, S. Wang and D. a. Yang, *Chem. Eng. J.*, 2022, **428**, 132644.